7 Paper 2

Abrupt Increase in Permafrost Creep Rates Following Climate Change

HARALD ØVERLI ERIKSEN[1,2], TOM RUNE LAUKNES[1], LINE ROUYET[1], IVAR BERTHLING[3], KETIL ISAKSEN[4], HEIDI HINDBERG[1], YNGVAR LARSEN[1], and GEOFFREY D. CORNER[2]

[1]Norut, P.O. Box 6434, NO-9294 Tromsø, Norway

[2]Department of Geoscience, UiT-The Arctic University of Norway, P.O. Box 6050, NO-9037 Tromsø, Norway

[3]Department of Geography, Norwegian University of Science and Technology, NO-7491 Trondheim, Norway

[4]Norwegian Meteorological Institute, Research and Development Department, P.O. Box 43 Blindern, NO-0313 Oslo, Norway.

Abstract

Rock glaciers are creeping ice/debris permafrost landforms[1-4] found in cold mountain environments all over the world. For more than a decade, a significant acceleration, and in some cases even collapse of rock glaciers has been documented in the European Alps[5-9]. This development has been attributed to higher permafrost temperatures[6,10] combined with increasing liquid water content[5], but the factors controlling this acceleration are not known in detail[7,11]. Importantly, a similar dynamic behaviour is still poorly documented outside of the Alps. Here we provide evidence for recent acceleration of a rock glacier located in an area of discontinuous permafrost in northern Norway, based on 62 years (1954–2016) of remote sensing data. Average surface velocity as measured from aerial orthophotos increases from ~0.5 m yr^{-1} (1954–1977) to ~3.6 m yr^{-1} (2006–2014). By using ground displacement measurements from radar satellites and aerial photography, we show an increase of maximum velocity from ~2.5 m yr^{-1} in 1995 to ~65 m yr^{-1} in 2016. During the 62-year period, annual air temperature rose by 1.8 °C, mean annual precipitation by 330 mm, and maximum annual snow depth increased by 58 %. The observed acceleration is thought to have been initiated by increasing ground temperatures and degrading permafrost. We also obtain the spatial velocity pattern from satellite remote sensing data, and from these results we propose that dynamically different parts of the rock glaciers are separated by shear zones. Our work demonstrates the value of satellite remote sensing in documenting the dramatic spatial and temporal evolution of permafrost landforms that otherwise often are inaccessible due to remote or steep/dangerous terrain. This research is relevant for understanding the impact of global warming related to degrading permafrost in mountainous environments, and for improving forecasting of future geohazards and reliable risk management.

Rock glaciers are striking landforms developed from cumulative deformation of ice/debris mixtures under permafrost conditions[1-3]. They form a common but not ubiquitous part of high alpine and polar slope systems, both terrestrial and extra-terrestrial[4]. Ground temperature influences the rheology of such ice/debris mixtures in a non-linear manner[5,6,12], but rock glaciers also respond dynamically to changes in sediment input[7]. Our study area is located in the northern part of Troms county in northern Norway, which has the highest density of rock glaciers in Norway[13]. This study focuses particularly on one among many rock glaciers on the southwest-facing slope of Ádjet mountain in the Skibotn valley (Figure 1). The lobe ranges in elevation from ~690 to 1080 meters above sea level (m a.s.l.), close to the regional altitudinal limit of mountain permafrost, according to borehole temperature data and modelling[14]. In front of the lobe, scree aprons reach down to 580 m a.s.l. (Figure 1 inset). The rock glacier has developed from rockslide talus beneath a ~200 m high, sub-vertical and highly fractured headwall consisting of quartz-rich and garnet-mica-schist. The lobe has longitudinal and transverse furrows, often with snow-filled depressions. The deepest depression is ~16 m deep, located on the gently sloping middle part of the lobe (~880 m a.s.l.). On the neighbouring lobe to the south we observed a thermokarst lake with visible bottom ice during the summers of 2015 and 2016. Ground temperature measurements in pore spaces in the active layer gave mean annual temperatures of -1.8 °C in 2014 and -3.4 °C in 2015, indicating permafrost conditions.

We found decadal velocity variations by manually tracking the position of large blocks identified in aerial orthophoto stereopairs from 1954, 1977, 2006 and 2014 (Figure S1). The rock glacier front advanced by ~180 m and one internal lobe front advanced by ~100 m between 1954 and 2014 (Figure 1, Figure S2). To characterize the surface stability in the surrounding area at higher spatial and temporal resolution, we applied offset-tracking[15-18] and interferometric (InSAR)[19,20] techniques to a high-resolution TerraSAR-X satellite synthetic aperture radar (SAR) remote sensing dataset, covering the period from 2009–2016. We also estimated the velocity by computing a radar interferogram from 22.–23. July 1995, using SAR data from the European Space Agency ERS-1 and ERS-2 satellites. Mean annual velocities along the radar Line-of-Sight (LOS) direction show debris from the foot of the headwall supplying the rock glacier lobe with material having velocities of up to 0.15 m yr^{-1} (Figure 1).

Displacement rates on the rock glacier lobes are too high to be measured using satellite InSAR due to phase decorrelation. In order to detect annual displacement rates at the m yr^{-1}

level, we averaged many TerraSAR-X offset-tracking pairs for each year, using both ascending and descending geometries. We also carried out two campaigns using terrestrial radar interferometry[21,22] (TRI) (August 2014 and May 2015). TRI provides minute-scale surface displacement information, but for this study we have focused on averaged trends during the campaigns. To investigate spatial and temporal displacement patterns we project the TerraSAR-X offset-tracking and ERS InSAR displacement onto a selected profile along the rock glacier (Figure 2a). Offset-tracking results show a maximum surface parallel flow of ~65 m yr^{-1} in the lower part, and ~5 m yr^{-1} in the upper part of the rock glacier during the snow-free season of 2016. This is an increase of 2500% on the lower lobe and 400% on the upper, compared to velocities observed by the July 1995 1-day ERS interferogram. Velocity is lowest in the middle part of the rock glacier (~750 m in profile A-A’, Figure 2a, Figure S2 and S3). The lower part shows acceleration, except for the 2009–2010 period. The upper part accelerates from 1995–2009, decelerates from 2009–2011, and then accelerates during 2012–2016. Recent acceleration in the upper part is delayed with respect to the lower part (Figure 2a). This can be a response to debuttressing caused by the speed-up of the lower part. Deformation may be taking place along internal shear zones, retrogressively extending higher up on the rock glacier (see time-lapse movie of TerraSAR-X backscatter in Supplementary Information). Similar dynamics is described by Gorbunov, et al. [23] for the Burkutty rock glacier and by Hartl, et al. [24] for the Outer Hochebenkar rock glacier.

In order to compare decadal (aerial orthophoto), single year (TerraSAR-X offset-tracking), seasonal (TRI), and single day (ERS InSAR) displacement rates, we computed spatial velocity averages for an area on the lower part of the rock glacier (Figure 1 and projected the displacements onto the profile A-A' (Figure 2b). Velocities are increasing on a decadal scale, with a recent acceleration. Velocities from the 1-day ERS interferogram in July 1995 confirm the trend from the 1977–2006 orthophoto comparison, indicating reliability in decadal displacement. A similar comparison between TRI and SAR offset-tracking confirms the recent very high yearly velocities, and TRI results also point to variability in seasonal displacements with higher velocities in summer 2014 than in spring 2015 (Figure S5). The extrapolation of the 1-day July 1995 ERS InSAR velocity is probably overestimated due to such seasonal variations in rock glacier velocity[25].

Climate has changed during the 62-year timespan covered by the remote sensing data. Based on daily gridded air temperature and precipitation data at 1 km^2 resolution[26] the analyses show an increase in mean annual air temperature (MAAT) of 1.8 °C during this period and annual precipitation increased of 330 mm. Moreover, the maximum annual snow depth increased by 58 % (Figure 2c-e). The gridded MAAT data were verified using 667 days of local air temperature observations at 1024 m a.s.l. from Ádjet (Figure 2c). Regional observed trends in permafrost temperatures in northern Scandinavia show accelerating warming since 2000[27] with a change in mean annual ground temperature of between +0.1 and +0.4 °C/decade[28]. Finally, permafrost degradation was observed recently in an instrumented borehole ca. 30 km east of Ádjet[14]. Combined, these results suggest increasing permafrost temperatures within the rock glacier body.

To understand the rock glacier kinematics, we calculated the longitudinal strain rate along the profile A-A' for individual years. Direct strain rate calculations from velocity data are inherently sensitive to velocity errors[29], and we used spatially averaged velocities to mitigate this problem. The most noticeable kinematic signal is the pulse from extension to compression within the lower part of the rock glacier (~300 m profile A-A', Figure 3a). The extension increased from 1995 to 2016 in the area where the rock glacier moves over convex terrain. We hypothesize that this is the surface displacement signal of the high velocity lower part being disconnected from the slower moving upper part. Further towards the front, compression has been steadily increasing from 1995 to 2016 (Figure 3a). In the low velocity upper part there are small scale variations in strain rate related to slope gradient, especially across transverse ridges and internal lobe fronts (~800 m and ~1050 m in profile A-A') (Figure 3a, d).

To further explore the displacement pattern of the rock glacier, we identified areas with displacement into the ground (thinning) and out of the ground (thickening) (Figure 3b) by combining SAR offset-tracking velocities from both TerraSAR-X ascending and descending geometries[19]. We observe a general trend of thinning in the upper part and alternation between thickening and thinning in the middle and lower part. The spatial and temporal pattern of thinning and thickening is relatively constant over time, but a new zone of thickening appears at ~650 m from 2011. These zones coincide with areas of the rock glacier where slope is increasing, and may thus be advancing internal lobes (Figure 3d).

Velocities recorded in the lower part of the Ádjet rock glacier exceed the empirical model considered by Kääb, et al. [6] by an order of magnitude. Following their approach further, using a maximum rock glacier thickness of 35 m, an overall density of 1900 kg/m^3, a spatially averaged surface slope of 30° and an *A* value for temperate ice, provides a surface velocity estimate of ~64 m yr^{-1} based on Glen's flow law. Our recorded velocities could thus potentially be explained by internal deformation alone, but other factors may also contribute. Especially, the rapid changes in velocities in both time and space point to explanations beyond rheological considerations even considering the strong non-linearity in constitutive relationships. Similar to the destabilized rock glaciers in Mattertal[30], the Ádjet rock glacier moves over an underlying bedrock topography that causes a convex break in slope. Such topography may be a controlling factor for the observed spatial pattern of extension and compression. The depression at ~700 m may be similarly related to an underlying shear zone extending towards the surface, as was documented Merz, et al. [31] from the Furggwanghorn rock glacier. It most likely formed due to the observed extension, and may have played an important role in triggering the acceleration. Conditioned by increasing air temperatures, precipitation and snow depth[5,32] and stretching of the permafrost body (increasing thermal gradients), increased deformation from warm permafrost may have started a positive feedback process where infiltrating water from precipitation[25] and melting snow could contribute to elevated pore water pressures along internal shear zones and/or potentially a basal detachment. Such factors could help explaining the evolution of the deformation.

So far we have no data directly describing subsurface conditions and thermal properties for the Ádjet rock glacier. Nevertheless, our detailed remote sensing information of surface displacements suggests that the rock glacier's kinematics are related to normal and reverse shear zones, that the rock glacier has areas that stretch or compress, and areas that increases or decreases in thickness. This provides an additional dynamic element to the surface parallel shear zone described for many alpine rock glaciers[3,33] (Figure 3c). It is also in line with recent results combining geophysical surveys and borehole inclinometer measurements[34]. Depending on the reaction to future climate forcing, the implication of degrading permafrost could have severe consequences for infrastructure and settlements in mountainous regions having a high density of rock glaciers, due to e.g. increased debris flow activity [35]. As permafrost landforms often are located in inaccessible, rough terrain, placing in-situ instrumentations is costly and often dangerous. Our remote sensing approach in conjunction with increased availability of satellite radar remote sensing systems, e.g. Sentinel-1 from the EU Copernicus programme, could help fulfil an urgent need to monitor the consequences of climate change[11]. The ability to investigate large areas and the upscaling of site-specific multimethod geophysical and geotechnical investigations[31,36], could pave the way for an improved understanding, and more detailed monitoring, exploration and early warning related to future degrading permafrost.

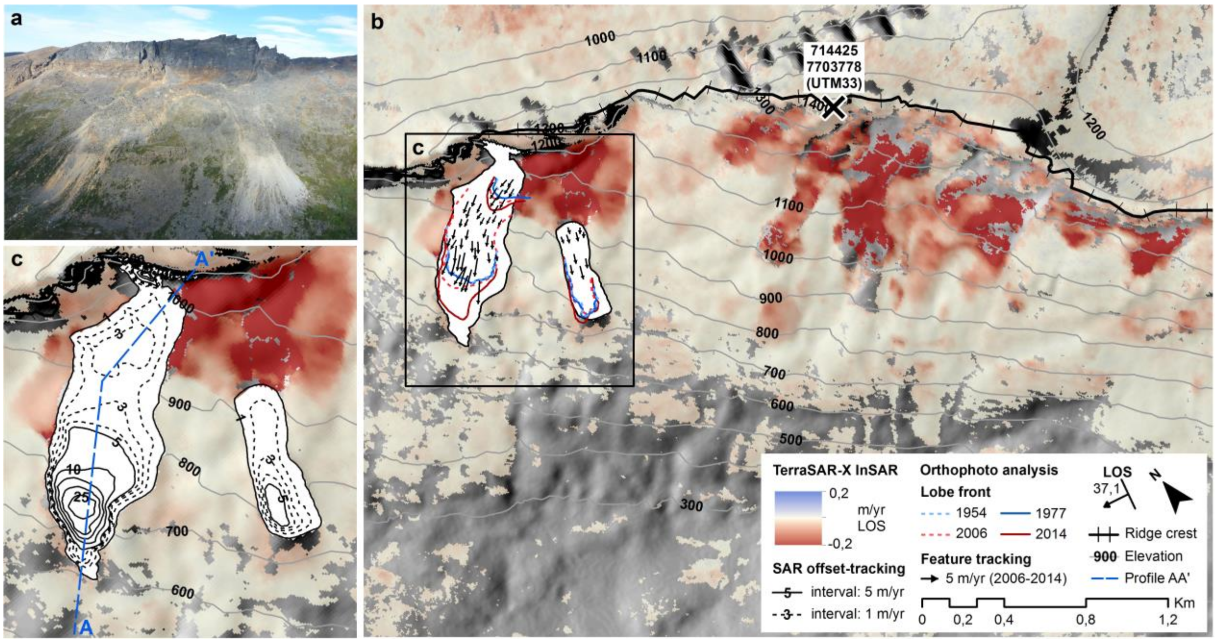

Figure 1 | Ground displacements in the Ádjet rock glacier complex. **a.** Aerial photo close-up of the two most active rock glacier lobes (NGU, 2013). **b.** Overview of ground surface LOS mean velocities observed by TerraSAR-X InSAR (2009–2016). Red areas indicate active slope processes with deformation away from the satellite (downward and westward). We focus on the most active rock glaciers in the northwestern area, indicated by the black rectangle. Here, orthophoto analysis using aerial images since 1954 allow tracking of the lobe positions and other observable features. **c.** Deformation with rates up to several m yr^{-1} is detected using SAR offset-tracking. The location of the profile A–A' is marked in **c**. Figure background is shaded relief from 10 m resolution DEM.

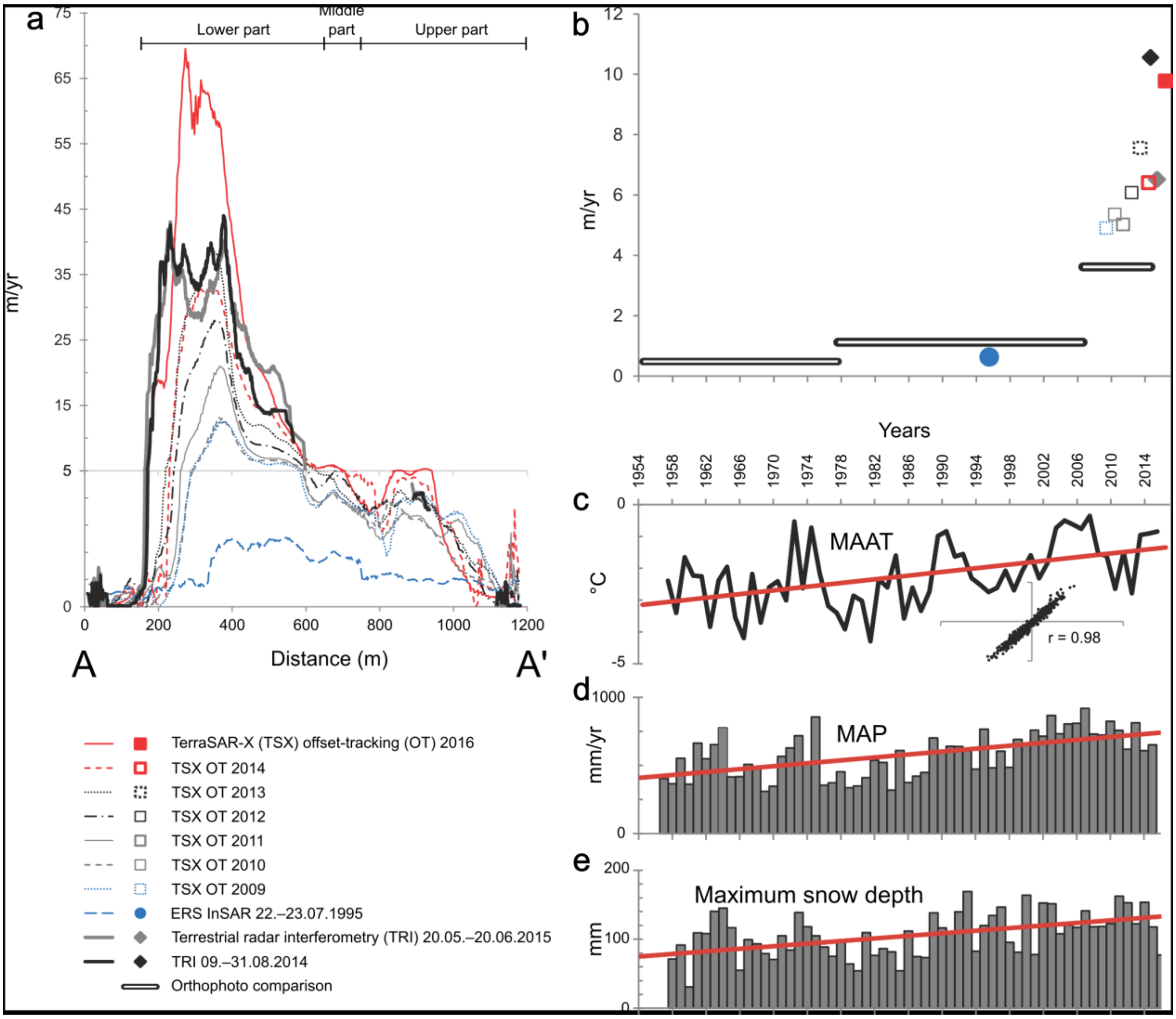

Figure 2 | Spatial and temporal variations of displacement rates of Ádjet rock glacier compared to modelled local climate data. a. Surface parallel yearly velocity in profile A–A' from TerraSAR-X offset-tracking (2009–2016) and ERS InSAR (one interferogram in July 1995). Note the break in the vertical scale at 5 m yr^{-1}. **b.** Comparison of mean yearly horizontal velocity for area in middle part of the rock glacier from orthophotos, terrestrial- and satellite-based radar data. **c.** Mean annual air temperature (MAAT) (1954–2014). Inset shows gridded daily temperature compared to locally observed temperature over 677 days at Ádjet. **d.** Mean annual precipitation (MAP). **e.** Maximum snow depth. Red lines show linear trend of climatic data from 1957–2016. Climatic data is from (SeNorge.no).

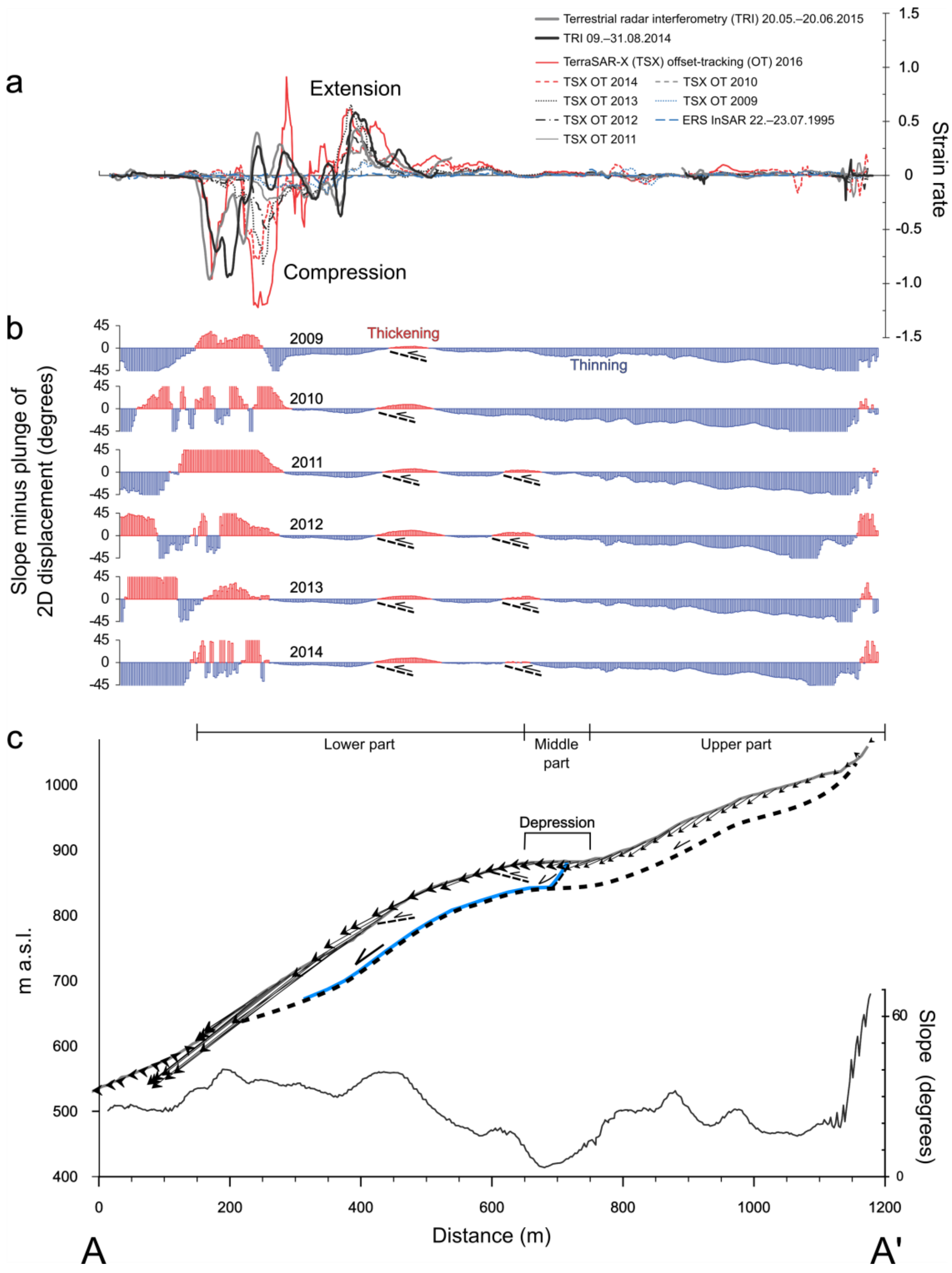

Figure 3 | Kinematic variation along profile A–A' from radar remote sensing data. a. Spatial and temporal variations of strain rate from individual years based on surface parallel flow from range component of TerraSAR-X offset-tracking (2009–2016), LOS velocity from ERS InSAR (July 1995), and LOS velocities from TRI (2014 and 2015). **b**, Annual variations in tinning and thickening calculated by subtracting slope from plunge of 2D offset-tracking surface displacement vectors. **c**, Geological model with terrain surface and terrain slope.

Vectors indicate surface velocity and plunge from 2D offset-tracking. Depression and possible zone of elevated pore pressures (blue line) due to infiltration of water are marked. Basal detachment to bedrock is interpreted from surrounding outcrops (dashed line).

References

1 Berthling, I. Beyond confusion: Rock glaciers as cryo-conditioned landforms. *Geomorphology* **131**, 98-106, doi:dx.doi.org/10.1016/j.geomorph.2011.05.002 (2011).

2 Barsch, D. *Rockglaciers. Indicators for the Present and Former Geoecology in High Mountain Environments*. 331 (Springer Verlag, Heidelberg, 1996).

3 Haeberli, W. *et al.* Permafrost creep and rock glacier dynamics. *Permafrost and Periglacial Processes* **17**, 189-214, doi:dx.doi.org/10.1002/ppp.561 (2006).

4 Head, J. W. *et al.* Tropical to mid-latitude snow and ice accumulation, flow and glaciation on Mars. *Nature* **434**, 346-351, doi:doi:10.1038/nature03359 (2005).

5 Ikeda, A., Matsuoka, N. & Kääb, A. Fast deformation of perennially frozen debris in a warm rock glacier in the Swiss Alps: An effect of liquid water. *Journal of Geophysical Research* **113**, doi:10.1029/2007jf000859 (2008).

6 Kääb, A., Frauenfelder, R. & Roer, I. On the response of rockglacier creep to surface temperature increase. *Global and Planetary Change* **56**, 172-187, doi:dx.doi.org/10.1016/j.gloplacha.2006.07.005 (2007).

7 Müller, J., Vieli, A. & Gärtner-Roer, I. Rock glaciers on the run – understanding rock glacier landform evolution and recent changes from numerical flow modeling. *The Cryosphere* **10**, 2865-2886, doi:10.5194/tc-10-2865-2016 (2016).

8 Bodin, X. *et al.* The 2006 Collapse of the Bérard Rock Glacier (Southern French Alps). *Permafrost and Periglacial Processes* **28**, 15, doi:10.1002/ppp.1887 (2016).

9 Noetzli, J., Luethi, R. & Staub, B. PERMOS 2016. Permafrost in Switzerland 2010/2011 to 2013/2014. *Glaciological Report (Permafrost) No. 12-15 of the Cryospheric Commission of the Swiss Academy of Sciences*, 85 (2016).

10 Roer, I., Kääb, A. & Dikau, R. Rockglacier acceleration in the Turtmann valley (Swiss Alps): Probable controls. *Norsk Geografisk Tidsskrift - Norwegian Journal of Geography* **59**, 157-163, doi:10.1080/00291950510020655 (2005).

11 Haeberli, W. *et al.* Mountain permafrost: development and challenges of a young research field. *Journal of Glaciology* **56**, 1043-1058, doi:10.3189/002214311796406121 (2010).

12 Moore, P. L. Deformation of debris-ice mixtures. *Reviews of Geophysics* **52**, 435-467, doi:10.1002/2014RG000453 (2014).

13 Lilleøren, K. S. & Etzelmuller, B. A regional inventory of rock glaciers and ice-cored moraines in Norway. *Geografiska Annaler* **93**, 175-191, doi:doi.org/10.1111/j.1468-0459.2011.00430.x (2011).

14 Farbrot, H., Isaksen, K., Etzelmuller, B. & Gisnas, K. Ground Thermal Regime and Permafrost Distribution under a Changing Climate in Northern Norway. *Permafrost and Periglacial Processes* **24**, 20-38, doi:Doi 10.1002/Ppp.1763 (2013).

15 Erten, E., Reigber, A. & Hellwich, O. Generation of three-dimensional deformation maps from InSAR data using spectral diversity techniques. *ISPRS Journal of Photogrammetry and Remote Sensing* **65**, 388-394, doi:dx.doi.org/10.1016/j.isprsjprs.2010.04.005 (2010).

16 Strozzi, T., Luckman, A., Murray, T., Wegmuller, U. & Werner, C. L. Glacier motion estimation using SAR offset-tracking procedures. *IEEE Transactions on Geoscience and Remote Sensing* **40**, 2384-2391, doi:10.1109/TGRS.2002.805079 (2002).

17 Sund, M., Lauknes, T. R. & Eiken, T. Surge dynamics in the Nathorstbreen glacier system, Svalbard. *The Cryosphere* **8**, 623-638, doi:10.5194/tc-8-623-2014 (2014).

18 Rignot, E., Mouginot, J. & Scheuchl, B. Ice Flow of the Antarctic Ice Sheet. *Science* **333**, 1427-1430 (2011).

19 Eriksen, H. Ø. *et al.* Visualizing and interpreting surface displacement patterns on unstable slopes using multi-geometry satellite SAR interferometry (2D InSAR). *Remote Sensing of Environment* **191**, 297-312, doi:dx.doi.org/10.1016/j.rse.2016.12.024 (2017).

20 Lauknes, T. R. *et al.* Detailed rockslide mapping in northern Norway with small baseline and persistent scatterer interferometric SAR time series methods. *Remote Sensing of Environment* **114**, 2097-2109, doi:dx.doi.org/10.1016/j.rse.2010.04.015 (2010).

21 Caduff, R., Schlunegger, F., Kos, A. & Wiesmann, A. A review of terrestrial radar interferometry for measuring surface change in the geosciences. *Earth Surface Processes and Landforms* **40**, 208-228, doi:10.1002/esp.3656 (2015).

22 Werner, C., Strozzi, T., Wiesmann, A. & Wegmuller, U. A Real-Aperture Radar for Ground-Based Differential Interferometry. *IGARSS 2008 - 2008 IEEE International*

Geoscience and Remote Sensing Symposium **3**, III - 210-III - 213, doi:10.1109/IGARSS.2008.4779320 (2008).

23 Gorbunov, A. P., Titkov, S. N. & Polyakov, V. G. Dynamics of rock glaciers of the Northern Tien Shan and the Djungar Ala Tau, Kazakhstan. *Permafrost and Periglacial Processes* **3**, 29-39, doi:10.1002/ppp.3430030105 (1992).

24 Hartl, L. E. A., Fischer, A., Stocker-Waldhuber, M. & Abermann, J. Recent speed-up of an alpine rock glacier: an updated chronology of the kinematics of outer hochebenkar rock glacier based on geodetic measurements. *Geografiska Annaler: Series A, Physical Geography* **98**, 129-141, doi:10.1111/geoa.12127 (2016).

25 Wirz, V. *et al.* Short-term velocity variations at three rock glaciers and their relationship with meteorological conditions. *Earth Surf. Dynam.* **4**, 103-123, doi:10.5194/esurf-4-103-2016 (2016).

26 Saloranta, T. M. Simulating snow maps for Norway: description and statistical evaluation of the seNorge snow model. *The Cryosphere* **6**, 1323-1337, doi:10.5194/tc-6-1323-2012 (2012).

27 Isaksen, K., Sollid, J. L., Holmlund, P. & Harris, C. Recent warming of mountain permafrost in Svalbard and Scandinavia. *Journal of Geophysical Research: Earth Surface* **112**, F02S04, doi:10.1029/2006JF000522 (2007).

28 Romanovsky, V. E. *et al.* Terrestrial permafrost [in "State of the Climate in 2015"]. **97 (8)**, 149-152 (2016).

29 Kaab, A., Haeberli, W. & Gudmundsson, G. H. Analysing the creep of mountain permafrost using high precision aerial photogrammetry: 25 years of monitoring Gruben Rock Glacier, Swiss Alps. *Permafrost and Periglacial Processes* **8**, 409-426 (1997).

30 Delaloye, R. *et al.* in *Jahrestagung der Schweizerischen Geomorphologischen Gesellschaft* (ed C. Graf) 21–31 (2013).

31 Merz, K. *et al.* Multidisciplinary geophysical investigations over an alpine rock glacier. *GEOPHYSICS* **81**, WA147-WA157, doi:10.1190/geo2015-0157.1 (2016).

32 Goodrich, L. E. The influence of snow cover on the ground thermal regime. *Canadian Geotechnical Journal* **19**, 421-432, doi:10.1139/t82-047 (1982).

33 Arenson, L., Hoelzle, M. & Springman, S. Borehole deformation measurements and internal structure of some rock glaciers in Switzerland. *Permafrost and Periglacial Processes* **13**, 117-135, doi:10.1002/ppp.414 (2002).

34 Merz, K., Green, A. G., Buchli, T., Springman, S. M. & Maurer, H. A new 3-D thin-skinned rock glacier model based on helicopter GPR results from the Swiss Alps. *Geophysical Research Letters* **42**, 4464-4472 (2015).

35 Krainer, K., Mussner, L., Behm, M. & Hausmann, H. Multi-disciplinary investigation of an active rock glacier in the sella group (Dolomites; Northern Italy). *Austrian Journal of Earth Sciences* **105**, 48-62 (2012).

36 Springman, S. M. *et al.* Multidisciplinary investigations on three rock glaciers in the swiss alps: legacies and future perspectives. *Geografiska Annaler: Series A, Physical Geography* **94**, 215-243, doi:10.1111/j.1468-0459.2012.00464.x (2012).

Acknowledgements

TerraSAR-X satellite data were provided by DLR (projects GEO0565, GEO0764, and GEO2497). ERS data were provided by ESA (project AOPOL.4104). Funding for H.Ø.E. was provided by a grant from Troms County Council. Development of the Norut InSAR processing chain has been supported by the Norwegian Space Centre via the Geohazard project, by the Research Council of Norway via the PermaSAR project, and by ESA via the PRODEX Permasat project. The authors would like to acknowledge support from Bjørn Barstad (Terratec) for preparing the orthophotos from 1954 and 1977. We thank Markus Eckerstorfer, Ole Patrick Larsen, and Aleksander Amundsen for the helping during field campaigns. We are grateful to Norwegian Geological Survey for help regarding logistics, to Iselin Bakkhaug and Hannah Nopper for setting out temperature loggers, and to Stein Rune Karlsen for supplying us with tripods. We acknowledge Øyvind Ørnebakk who cleared the forest in Skibotn during the terrestrial-based radar campaigns, and Pål Tengesdal and the rest of the gang in the Tromsø Astronomy Association for letting us stay in their comfortable Skibotn Observatory during field work.

Author contributions

H.Ø.E. formulated the idea and together with T.R.L. designed the analytical approach. H.Ø.E. and T.R.L. led the writing of the manuscript with all co-authors commenting. H.Ø.E. did the processing of the ERS satellite SAR data, orthophoto comparison, calculations to find variation in strain rate and areas of thickening/thinning, field work and in-situ instrumentation regarding ground temperature, and air temperature measurements, preparation of in-situ and modelled climatic data. T.R.L. did the offset tracking of the TerraSAR-X satellite SAR data. L.R. processed the InSAR from TerraSAR-X satellite SAR data. H.H., Y.L and L.R. processed the terrestrial radar data. I.B. contributed to data interpretation and performed analysis using Glen's flow law. K.I. supplied modelled local gridded climate data (mean annual air temperature, mean annual precipitation, and maximum annual snow depth), and interpretation regarding local and regional effects on ground temperature. G.D.C. contributed to data interpretation and pointed out the study area after years of field observations. All co-authors contributed to the manuscript.

Additional information

See the supplementary information available in a separate document.

Competing financial interests

The authors declare no competing financial interests.

Methods:

Abrupt Increase in Permafrost Creep Rates Following Climate Change

HARALD ØVERLI ERIKSEN[1,2], TOM RUNE LAUKNES[1], LINE ROUYET[1], IVAR BERTHLING[3], KETIL ISAKSEN[4], HEIDI HINDBERG[1], YNGVAR LARSEN[1], and GEOFFREY D. CORNER[2]

[1]Norut, P.O. Box 6434, NO-9294 Tromsø, Norway

[2]Department of Geoscience, UiT-The Arctic University of Norway, NO-9037 Tromsø, Norway

[3]Department of Geography, Norwegian University of Science and Technology, NO-7491 Trondheim,

Aerial orthophotos. Ortho-rectified aerial images acquired in 1954, 1977, 2006, and 2014 were used for feature tracking for velocity measurements and compilation of front positions. Comparison of the orthophotos enabled us to assess the accuracy. For this assesment the position of 13 objects (typically boulders) visible in all orthophotos were measured and compared. To minimise the effects of dependencies between the orthophotos none of the used ground-control-points (GCP) were chosen, furthermore to minimise errors and bias from using objects having potentially moved over the years between the dates of photography the objects were located in areas assumed to be stable. This assessment may be seen as a check of the relative fit between the orthophotos outside the area of interest thus making it possible to consider the underlying uncertainties and thereby increasing the reliability of the measurements of relative movements used in this study. Accuracy of orthophotos is estimated to be on the order of 1 m (root mean square error) for well-defined features.

SAR offset-tracking. We used 75 TerraSAR-X StripMap mode scenes from descending geometry, spanning the period from 2009 to 2016 (minus 2015). We used a cross-correlation-based method to estimate range and azimuth offsets between pairs of SAR data acquired in the same geometry[12-14], allowing a temporal baseline of 22–44 days. The input SAR data were coregistered to a reference geometry, and the range and azimuth shifts were estimated by searching for the maximum of the two-dimensional correlation function estimated by using rectangular matching window sizes uniformly distributed over the image frame. The quality of the estimates is provided by the signal-to-noise ratio (SNR), which is the ratio between the correlation peak and the average level outside the search region. We masked out the points with low SNR and removed outliers by applying a median filter. For each year, we then averaged (stacked) all offset-fields, providing an estimate of annual velocity fields, measured in the plane spanned by the range and azimuth vectors. The surface-parallel flow approximation was used to project the range and azimuth velocities onto the downslope direction, using a profile along the rock glacier.

Interferometric synthetic aperture radar (InSAR). InSAR results were produced using the Norut GSAR software[1]. By using TerraSAR-X StripMap snow-free scenes (mainly between June and September) from descending geometry, we computed 49 multilooked interferograms with a short temporal baseline of 11 days. A spatial multilooking of 4 looks in range and 3 looks in azimuth provided pixels with a ground resolution of ∼6 x 6 m. Stratified atmosphere was estimated and removed using a phase delay elevation profile for each interferogram[2], before phase unwrapping using SNAPHU software[3]. We then averaged (stacked) all unwrapped interferograms, providing an estimate of average annual LOS velocity for the whole period 2009–2016. The ERS-1/2 tandem interferogram from 22.–23. July 1995 was produced using a multilooking of 2 looks in range and 8 looks in azimuth, providing a ground pixel resolution of ~40 x 30 m. An area with exposed bedrock was used to calibrate the InSAR phase. Low-coherence areas were masked out. A DEM from Norwegian Mapping Authority (10 m resolution) was used to remove the topographic phase contribution and for geocoding of the final results.

We stress that the InSAR method for surface displacement has certain limitations. The radar measures displacement in the line-of-sight (LOS) direction only, and sensitivity is thus zero in cases where the actual surface displacement vector is perpendicular to the LOS. Further, areas with severe surface displacement between the images used to form the interferogram will be decorrelated or will have phase ambiguities. This is the case for many areas on the rock glaciers using TerraSAR-X, which has 11 days revisit period. By using ERS-1/2 from the tandem-phase with 1-day revisit period, we are able to retrieve a phase signal also on the Adjet rock glacier.

As with offset-tracking the surface-parallel flow approximation was used to project the ERS LOS velocities onto the downslope direction, using a profile along the rock glacier.

Terrestrial radar interferometry (TRI). During 23 days in 2014, (09.08.–31.08), and 32 days in 2015 (20.05.–20.06), we scanned the mountain slope of Ádjet every 5 minutes using a Gamma Portable Remote Interferometer (GPRI). This is a real aperture radar with 2 m long rotating antennas. The system provides a ground resolution of ~8 x 0.75 m (azimuth/range) at 1 km distance[32] The GPRI was located at a distance of ~2.2 to 3.2 km from the rock glacier lobes.

From the acquired GPRI data we produced deformation time series and estimated mean annual velocities based on the total displacements at the end of the campaigns in order to be compared with the other datasets. The atmospheric signal was removed based on the assumption that atmosphere is correlated in space, and mainly uncorrelated in time except for the component correlating with altitude. GPRI data was calibrated to the same reference area as offset-tracking and InSAR data, and georeferenced to a ground resolution of 2 x 2 m.

As with offset-tracking and the ERS interferogram, the surface-parallel flow approximation was used to project the TRI velocities onto the downslope direction, using a profile along the rock glacier.

Climatic data. From gridded daily temperature, precipitation and snow cover[4] data (1957–2016) we compute mean annual air temperature (MAAT), mean annual precipitation (MAP), and maximum annual snow depth. Gridded data had 1 km^2 spatial resolution (http://www.senorge.no/). The gridded meteorological model data has a resolution of 1×1 km origin. Model data was extracted for an area closest to the rock glacier from an elevation of 852 m a.s.l. For comparison with modelled data we calculated MAAT based on air temperature measurement from 4 measurements per day, over 677 days, from two iButton loggers (16.08.2014–17.07.2015 and 25.08.2015–30.07.2016). The iButtons were mounted in a ventilated white plastic box, isolated from the box using small closed-cell foam pads. The box was mounted on a 1 m tall tripod, facing north, located on a large boulder at 1026 m a.s.l (34 W 479559 7691587) ~3.8 km SE of the rock glacier. To evaluate the ground thermal regime, we measured air temperature in fractures and pore space between large boulders. For this, we used iButtons mounted on plastic rods immersed into the open-work active layer.

Strain rate calculation. Strain rate or downslope acceleration and deceleration was calculated from TerraSAR-X offset-tracking (2009-2014, and 2016) displacement velocity from the descending orbit projected into the profiles slope and azimuth. Along the profile, we calculated the mean velocity gradient (strain rate) using a moving average of velocities from an area 40 meter orthogonal and ~10 meters parallel to the profile.

Kinematic calculation. Displacement patterns into the ground (thinning) and out of the ground (thickening) was calculated by combining SAR offset-tracking velocities from both TerraSAR-X ascending and descending geometries to two-dimensional (2D) surface displacement vectors[5]. Resulting 2D displacement vectors providing direction and magnitude for displacement in the vertical east-west plane were projected into the profile. By subtracting slope from the plunge of 2D displacement vectors along the profile, areas with displacement into the ground (subsidence) and out of the ground (uplift) could be identified.

Calculation of internal deformation. We assume that we can estimate the internal deformation of the rock glacier by using Glens flow law of ice. Then, surface velocity $U_s = A(\rho g \sin\alpha)^3(H/4)^4$, where A is a rate factor depending especially on temperature, ρ is the density of the deforming material, α is the surface slope and H is the total thickness of the material (e.g. Anderson and Anderson [6]).

1 Larsen, Y., Engen, G., Lauknes, T. R., Malnes, E. & Høgda, K. A. in *Proc. ESA Fringe 2005, ESA ESRIN, Frascati, Italy, November 28-December 2.*

2 Cavalié, O., Doin, M. P., Lasserre, C. & Briole, P. Ground motion measurement in the Lake Mead area, Nevada, by differential synthetic aperture radar interferometry time series analysis: Probing the lithosphere rheological structure. *Journal of Geophysical Research: Solid Earth* **112**, 18, doi:http://dx.doi.org/10.1029/2006JB004344 (2007).

3 Chen, C. W. & Zebker, H. A. Two-dimensional phase unwrapping with statistical models for nonlinear optimization. *Proceedings of the Geoscience and Remote Sensing Symposium, 2000.* **7**, 3213-3215, doi:10.1109/IGARSS.2000.860386 (2001).

4 Saloranta, T. M. Simulating snow maps for Norway: description and statistical evaluation of the seNorge snow model. *The Cryosphere* **6**, 1323-1337, doi:10.5194/tc-6-1323-2012 (2012).

5 Eriksen, H. Ø. *et al.* Visualizing and interpreting surface displacement patterns on unstable slopes using multi-geometry satellite SAR interferometry (2D InSAR). *Remote Sensing of Environment* **191**, 297-312, doi:dx.doi.org/10.1016/j.rse.2016.12.024 (2017).

6 Anderson, R. S. & Anderson, S. P. *Geomorphology: the mechanics and chemistry of landscapes*. (2010).

Supplementary information:

Abrupt Increase in Permafrost Creep Rates Following Climate Change

HARALD ØVERLI ERIKSEN[1,2], TOM RUNE LAUKNES[1], LINE ROUYET[1], IVAR BERTHLING[3], KETIL ISAKSEN[4], HEIDI HINDBERG[1], YNGVAR LARSEN[1], and GEOFFREY D. CORNER[2]

[1]Norut, P.O. Box 6434, NO-9294 Tromsø, Norway

[2]Department of Geoscience, UiT-The Arctic University of Norway, NO-9037 Tromsø, Norway

[3]Department of Geography, Norwegian University of Science and Technology, NO-7491 Trondheim,

Study Area

The area studied are part of a the highly active southwest facing slope of the Ádjet mountain (1408 m a.s.l.) in the Skibotn valley. The study area consists of Caledonian bedrocks thrusted over Precambrian basement rocks during the Caledonian orogeny in the Silurian[1,2]. Locally, geomorphological features debris fields, talus fan deposits, and slide blocks are widespread, and several generations of rock glaciers have been mapped[3,4].

Post-Caledonian brittle faults formed during rifting in the late Paleozoic, Mesozoic and early Cenozoic time periods[5], and later controlled late-Cenozoic landscape, uplift-subsidence, and glacial erosion forming the todays high–relief alpine topography[6]. Today's valleys and fjords in Troms region mostly follow the trends of the rift-margin faults[7-10]. Slide blocks and controlling structures at Ádjet are controlled by reactivation of old brittle faults[3].

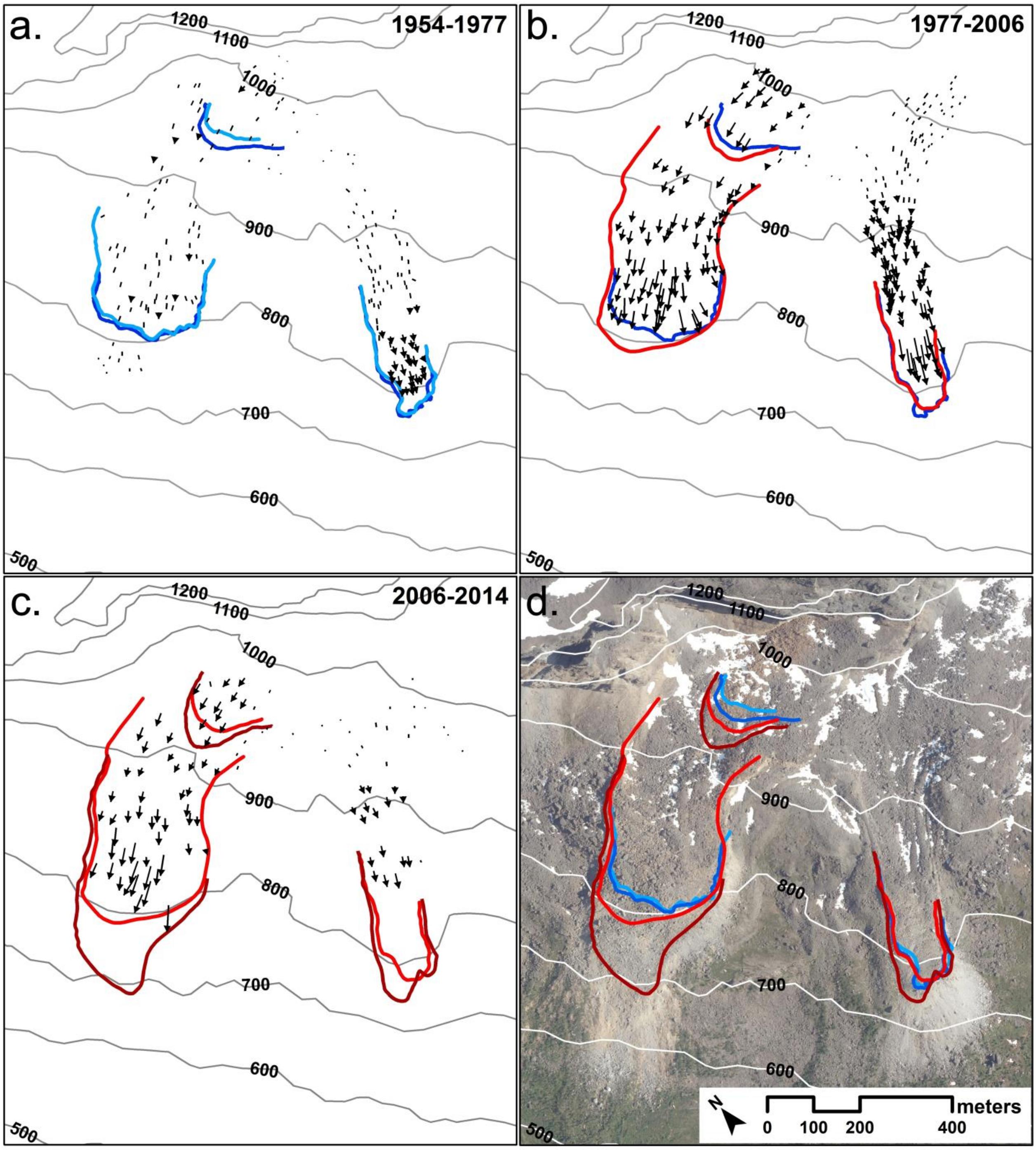

Figure S1 | Vector fields from orthophoto comparison. a, 1954–1977. **b,** 1977–2006. **c**, 2006–2014. **d,** Mapped front positions.

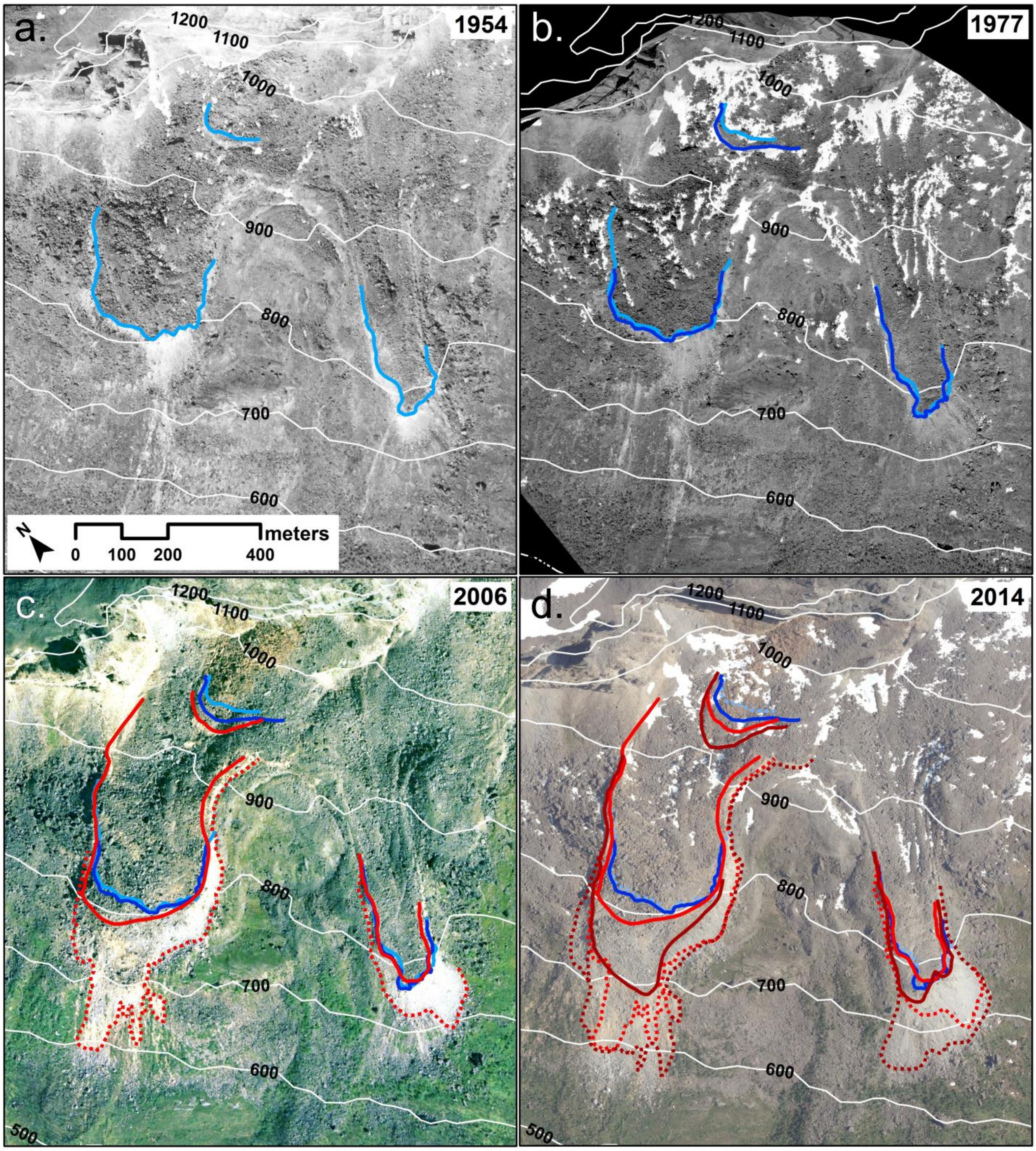

Figure S2 | High-resolution orthophoto of Ádjet rock glacier. a, 1954. **b,** 1977. **c**, 2006. **d,** 2014. Locations of interpreted lobe fronts (solid lines) and scree aprons (dashed lines) are indicated.

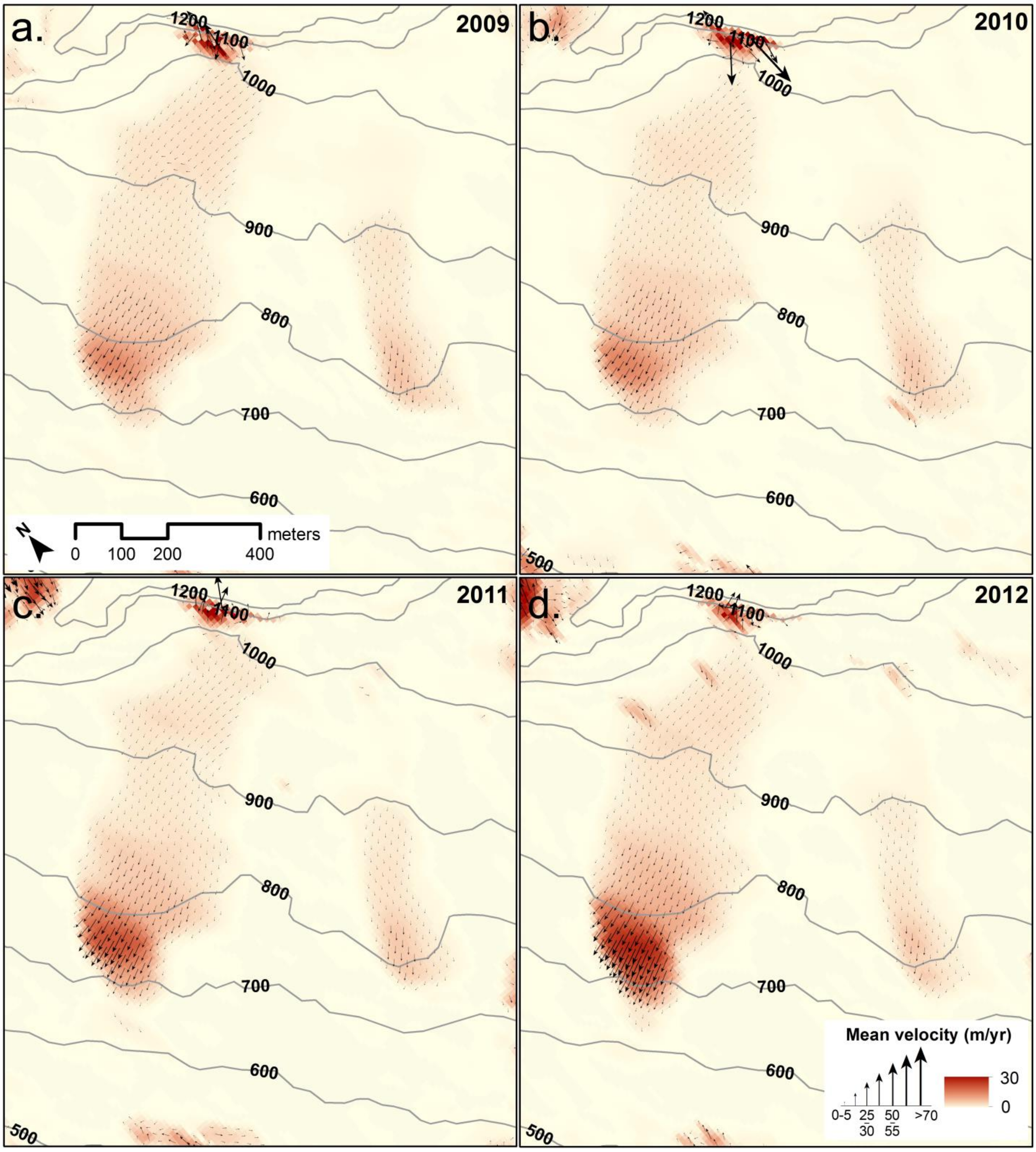

Figure S3 | Vector fields from SAR offset-tracking for the period 2009–2012. a, 2009. **b,** 2010. **c,** 2011. **d,** 2012. The vector fields are based on stacking (averaging) of pairs of SAR images obtained each summer season, with an allowed temporal baseline of 22–44 days. The background color indicated total deformation velocity.

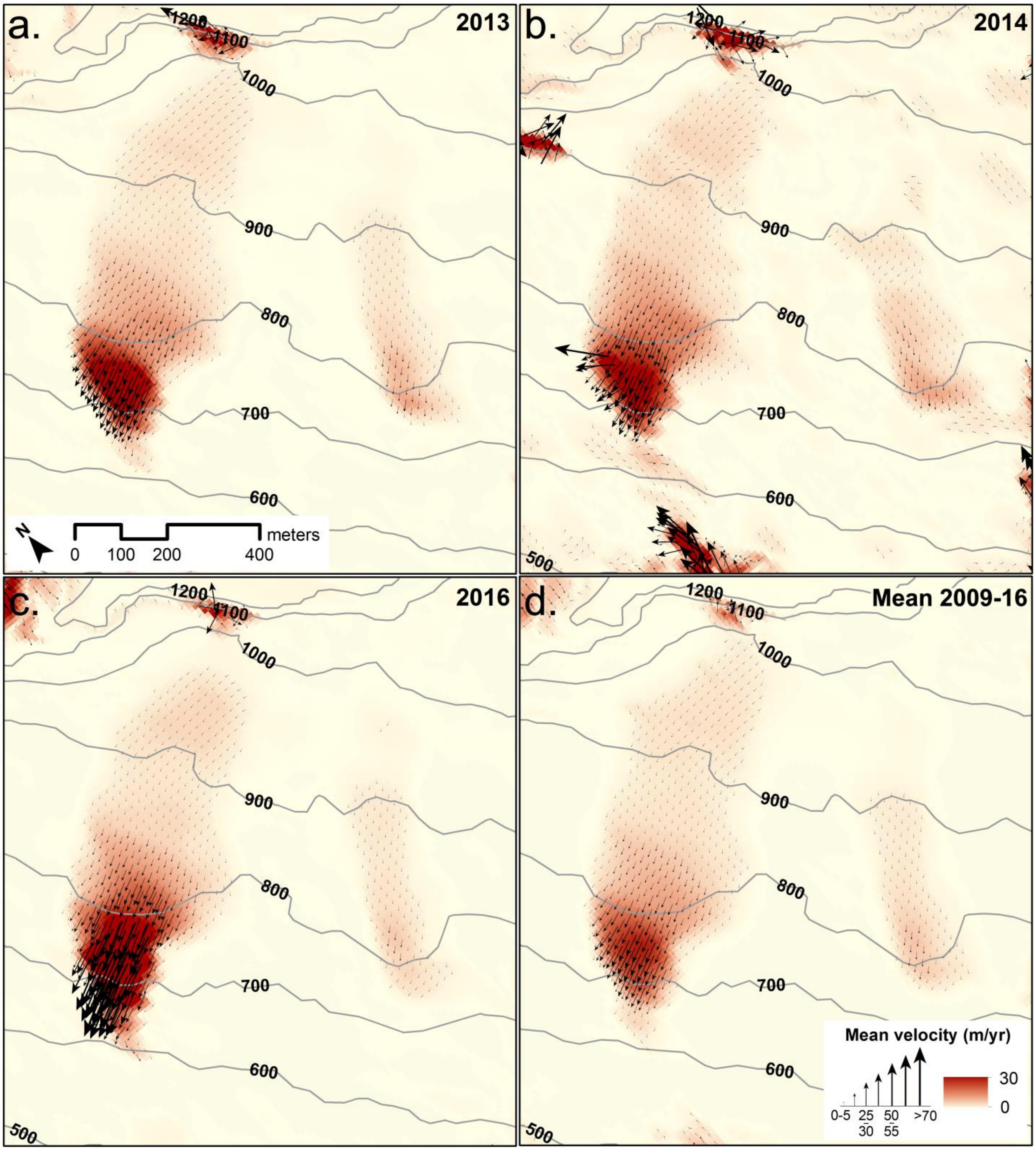

Figure S4 | Vector fields from SAR offset-tracking for the period 2013–2016. a, 2013. **b,** 2014. **c,** 2016. **d,** Average of period 2009–2016. The vector fields are based on stacking (averaging) of pairs of SAR images obtained each summer season, with an allowed temporal baseline of 22–44 days. The background color indicated total deformation velocity.

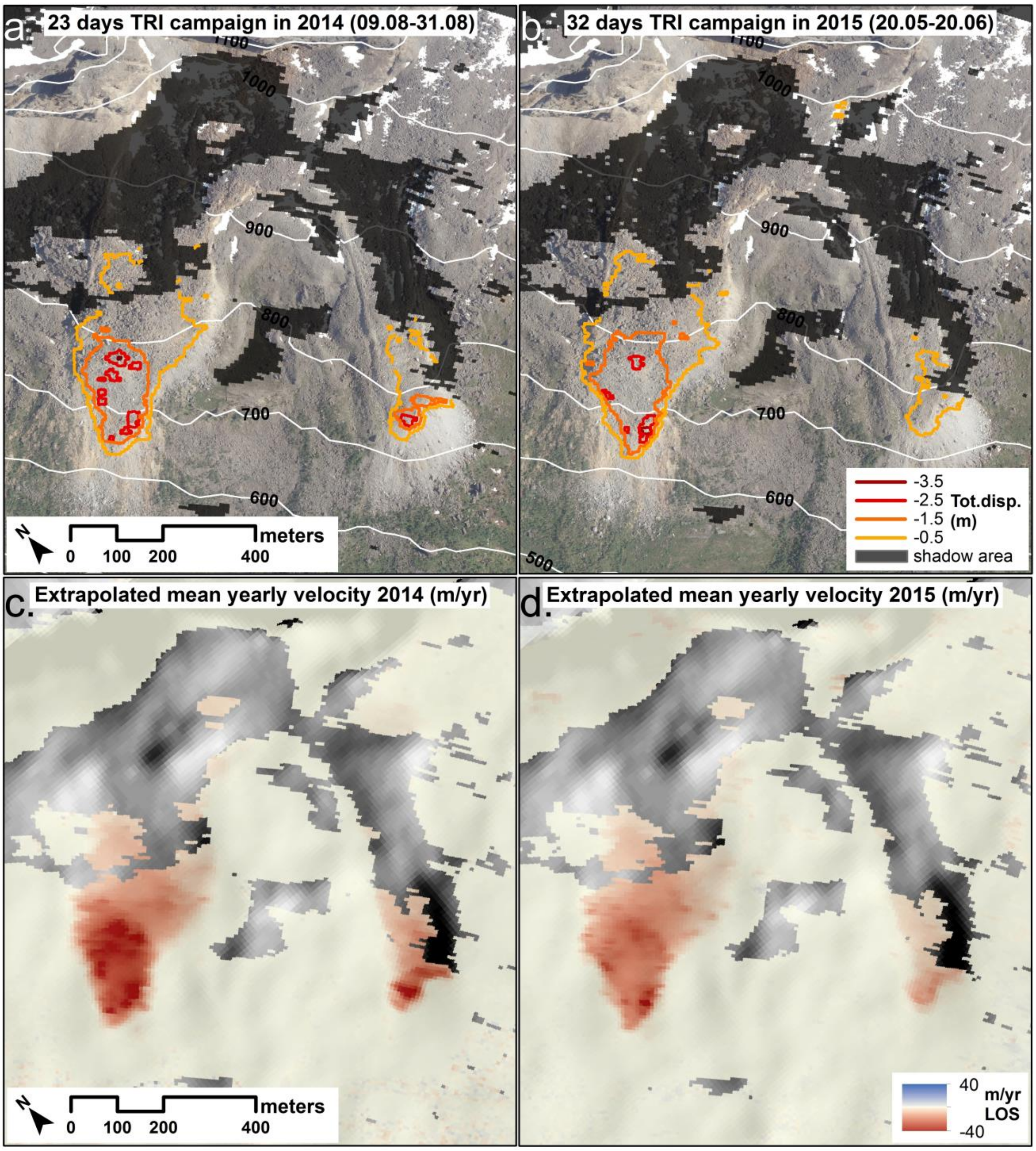

Figure S5 | Displacement field from terrestrial radar interferometry field campaigns. a, Total deformation during the 23 days long campaign in August 2014. **b,** Total deformation during the 32 days long campaign in May/June 2015. **c,** Extrapolated yearly velocity from 2014. **d,** Extrapolated yearly velocity from 2015. Deformation results are based on time-series InSAR processing of all 5. minute interval interferograms. Area affected by shadow is masked out.

References

1. Zwaan, K. B. Geologisk kart over Norge. Berggrunnskart NORDREISA - M 1:250 000, (in norwegian). *Norges geologiske undersøkelse* (1988).
2. Roberts, D. The Scandinavian Caledonides: event chronology, palaeogeographic settings and likely modern analogues. *Tectonophysics* **365**, 283-299, doi:dx.doi.org/10.1016/S0040-1951(03)00026-X (2003).
3. Bakkhaug, I. *Undersøkelse av ustabilt fjellparti ved Adjet, Storfjord, Troms. Betydningen av ulike kategorier av glideplan i berggrunnen og mekanismer for utglidning, Storfjord, Troms, Master thesis, University of Tromsø, Tromsø, Norway, (in norwegian)*, (2015).
4. Nopper, H. Geomorphological study of the rock-slope failure at Adjet, Storfjord, Troms, Unpublished Master Thesis, UiT-The Arctic University of Norway, Tromsø, Norway. 123 (2015).
5. Osmundsen, P. T., Sommaruga, A., Skilbrei, J. R. & Olesen, O. Deep structure of the Mid Norway rifted margin. *Norwegian Journal of Geology / Norsk Geologisk Forening* **82**, 205-224 (2002).
6. Corner, G. D. in *The Physical Geography of Fennoscandia. Oxford Regional Environments Series* (ed M. Seppälä) Ch. 229-254, (Oxford University Press, 2005).
7. Bergh, S. G. *et al.* The Lofoten-Vesterålen continental margin: a multiphase Mesozoic-Palaeogene rifted shelf as shown by offshore-onshore brittle fault-fracture analysis. *Norwegian Journal of Geology* **87**, 29-58 (2007).
8. Hansen, J. A., Bergh, S. G., Eig, K., Henningsen, T. & Olesen, O. Onshore-offshore basement architecture on the north Norwegian margin; influences of Mesozoic to early Palaeogene tectonics. *Proceedings of the EGU General Assembly* (2008).
9. Indrevær, K. *et al.* Post-Caledonian brittle fault zones on the hyperextended SW Barents Sea margin: New insights into onshore and offshore margin architecture. *NORWEGIAN JOURNAL OF GEOLOGY* **93**, 167- 188 (2013).
10. Hansen, J. A. & Bergh, S. G. Origin and reactivation of fracture systems adjacent to the Mid-Norwegian continental margin on Hamarøya, North Norway: use of digital geological mapping and morphotectonic lineament analysis. *Norwegian Journal of Geology* **92**, 391-403 (2012).